CHAPTER IV

HYSTERESIS AND OPTICAL BISTABILITY IN DEGENERATE FOUR-WAVE MIXING

A. Introduction

In the preceding chapter, we showed that the transmission of a distributed-feedback structure with an intensity-dependent refractive index displays hysteresis and bistability as the incident light intensity is varied. The feedback required for bistability is provided by Bragg scattering from periodic index variations built into the otherwise homogeneous medium. In the course of that work we noticed a striking similarity between the nonlinear DFB equations (Eqs. (3.20)) and those that describe the interaction of two pairs of counterpropagating waves in a nonlinear medium [1]. (This latter process known as degenerate four-wave mixing (DFWM) has attracted a great deal of attention recently because of its ability to compensate for phase distortions [2].) In fact if pump depletion is neglected a one-to-one correspondence can be made between the evolution of the forward and backward waves in the nonlinear DFB and that of the probe and signal waves in DFWM. We find similar coupling terms, the same purely reactive Kerr terms and the same boundary conditions, namely that the backward-propagat-

ing signals start with zero amplitude at the rear of the nonlinear medium. It became apparent that the mathematical similarity was indicative of the underlying physical connection between the two processes. In the nonlinear DFB structure, we recall that feedback is provided by Bragg scattering from periodic index variations built into the nonlinear medium. In the degenerate four-wave mixing process there is an internal "self-induced" feedback resulting from the instantaneous creation of gratings within the nonlinear medium by the interacting waves themselves. It was then natural to ask whether this combination of nonlinearity and feedback (albeit self-induced) could result in bistability in degenerate four-wave mixing. It is the purpose of this chapter to answer that question in the affirmative and to discuss the conditions under which bistability may be observed in DFWM.

In section B we review the relevant aspects of four-wave mixing with emphasis on the so-called grating picture of the interaction. We begin with the pioneering studies of Maker and Terhune [3] and point out the coherence length effect known as "Maker fringes." The recent work of Hellwarth [4] in connection with phase-conjugation is also discussed as well as observations of parametric amplification and oscillation.

Section C presents the nonlinear theory of degenerate four-wave mixing taking pump depletion and intensity-depend-

ent phase shifts into account. Exact analytic solutions to the coupled nonlinear equations are obtained.

The physical implications of these solutions are discussed in section D. Bistability is shown to be possible both in the reflected signal and in the spontaneous oscillation.

Finally in section E we offer suggestions for a possible experiment to observe the phenomena described herein.

We close this introductory section with some comments regarding possibly related investigations by other workers. After this work was done [5], we learned in a personal communication from V.S. Letokhov that he may have invented optical bistability in connection with a resonant-feedback laser based on a phase grating [6]. After a careful study of his paper we find that his system is quite different from ours. It consists of a laser with one standard Fabry-Perot mirror and another reflector which is a three-dimensional phase lattice created in a Kerr medium by the laser radiation itself. He finds that the combination of active medium and phase grating results in two possible output states for the field amplitude. He shows however that of these two states only one is stable. His system is therefore not bistable in the sense of having two stable stationary states for the same excitation conditions. In addition his analysis involves an active medium whereas our system is completely passive with only the parametric

coupling between pump and signal waves providing gain. A further search of the Russian literature has revealed some other interesting studies on the effects of self-induced feedback. Zeldovich [7], and Akhmanov and Lyakhov [8] have suggested that the anomalous gains and narrow spectral widths observed in stimulated Raman scattering may be due to the establishment of a "characteristic resonator" by distributed feedback. Lyakhov and Ponomarev [9] have done a numerical study of a DFB laser in which the feedback is established by the interfering pump waves. When the effects of gain saturation are taken into account they find a regime of hard self-excitation (hysteresis) when the pump parameter is varied. For the remainder of this chapter however we shall focus on bistability in a passive nonlinear medium.

B. Review of Four-Wave Mixing and Dynamic Grating Phenomena

The general interaction of four monochromatic waves in a nonlinear medium was studied theoretically [10] and experimentally [3] in the early days of nonlinear optics. The experiments of Maker and Terhune showed that the nonlinear susceptibility $\chi^{(3)}$ can couple three light waves together to generate a fourth. In those experiments a polarization at a frequency $\omega + \Delta$ and given by

$$P = \chi\left(-(\omega+\Delta),\ \omega,\omega,-(\omega-\Delta)\right)E(\omega)E(\omega)E^*(\omega-\Delta)e^{ik_{\omega+\Delta}z} \qquad (4.1)$$

was induced in the medium by waves at frequencies ω and $\omega - \Delta$. Then, assuming that the amplitudes of $E(\omega)$ and $E(\omega-\Delta)$ do not change much, the field at $\omega + \Delta$ is found from the wave equation to be

$$E(\omega+\Delta,z) = \frac{2\pi k_{\omega+\Delta}}{\varepsilon_{\omega+\Delta}} \chi\, E(\omega)E(\omega)E^*(\omega-\Delta)\frac{1-e^{i\Delta kz}}{\Delta k} \qquad (4.2)$$

where

$$\Delta k = 2k_{\omega} - k_{\omega+\Delta} - k_{\omega-\Delta}.$$

Physically, Δk measures the difference in phase between the polarization and the electric field generated at $\omega + \Delta$. One can define a coherence length

$$L_c = \pi/|\Delta k|$$

such that after a distance L_c, the polarization and the radiated field are 180° out of phase. Equation (4.2) shows that as the interaction length is varied, the intensity of the output wave oscillates with a period $2L_c$. It is these oscillations that are sometimes called Maker fringes. We will show later in this chapter that even when $\Delta k = 0$, intensity-dependent phase changes lead to analogous oscillatory behaviour.

Until recently, the interest in four-wave mixing was largely spectroscopic. The nonlinear susceptibility $\chi^{(3)}$

has resonances which are characteristic of the medium. These resonances can be probed by tuning the frequencies of the interacting waves and looking for an enhancement of the output. Spectroscopic techniques such as CARS (Coherent Anti-Stokes Raman Spectroscopy) and RIKES (Raman-Induced Kerr Effect Spectroscopy) utilize these resonances in $\chi^{(3)}$ [11].

Then in 1977 Hellwarth [4] pointed out that when counterpropagating pump beams are used, the four-wave mixing process can generate a signal wave whose complex amplitude is the complex conjugate to that of the probe wave. Such a phase conjugated wave could then be used to compensate for phase aberrations by sending it back through the same distorting medium traversed by the probe. Subsequently this prediction was verified experimentally by Jensen and Hellwarth [12], and by Bloom and Bjorklund [13] using CS_2 as the nonlinear medium. Since then there have been numerous reported observations of phase conjugate waves in both absorbing and transparent media.

Yariv has pointed out the similarity between degenerate four-wave mixing and real time holography [14]. In conventional holography one first records the hologram by exposing a photographic medium to the interference pattern between an object wave

$$a(x,y) = |a(x,y)| \exp[-j\phi(x,y)]$$

and a reference wave

$$A(x,y) = |A(x,y)|\exp[-j\psi(x,y)].$$

After developing, the amplitude transmittance of the film is proportional to

$$t(x,y) = |A|^2 + |a|^2 + A^*a + Aa^*$$

$$= |A|^2 + |a|^2 + 2|A||a|\cos(\phi(x,y) - \psi(x,y)) \tag{4.3}$$

If the hologram is now illuminated by the conjugate of the reference wave A^*, the grating term in $t(x,y)$ (the cosine term) serves to diffract this wave. The resulting field has a term of the form $|A|^2a^*$ which is proportional to the conjugate of the original object wavefront.

In four-wave mixing, the creation and reading-out of the hologram occur simultaneously. The nonlinear polarization that gives rise to the phase-conjugate wave is of the form

$$P_{NL} \sim \chi^{(3)}E_1E_2E_3^* ,$$

where E_1 and E_2 are counterpropagating pump waves and E_3 is a probe (object) wave. The object wave interferes with either of the pump waves and gratings are created through a modulation of the medium's properties (absorption or refractive index). These gratings then diffract the other pump wave to create the signal E_4.

The generation of phase-conjugate waves is actually incidental to the work to be discussed in this chapter. In fact, at the high conversion efficiencies considered here, the generated signal will not be a true replica of the object wave as a result of nonlinear phase distortions [15]. The important point is that transient gratings can be formed in various media due to the interference between light waves. Depending on the physical mechanism involved, these gratings can be of the phase (periodic variation of refractive index) or amplitude (periodic variation of the absorption) variety. In either case these gratings provide a feedback mechanism that leads to bistability.

C. The Nonlinear Theory of Degenerate Four-Wave Mixing

In this section we derive, and obtain analytic solutions for, the nonlinear coupled-wave equations that describe four-wave mixing in a Kerr medium. The model considered is that of Marburger and Lam [1] generalized to include a finite wave vector mismatch between the interacting waves. In the geometry of Fig. (4.1) two (nearly) counterpropagating pump waves E_1 and E_2 interact in a nonlinear medium with a probe wave E_3 to create a signal wave E_4 propagating in the opposite direction to E_3. To distinguish between the two sets of beams when the interaction is collinear, we assume that the pump beams are linearly polarized in the x-direction while the probe and signal are polarized along y.

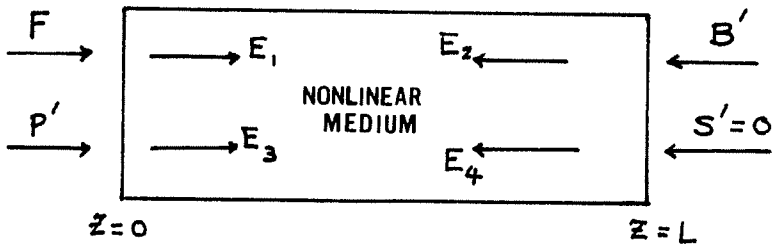

Fig. (4.1): Geometry of collinear DFWM. F and B' are pump fluxes, P' is the probe flux.

Furthermore we assume that the medium is lossless, the nonlinearity is instantaneous and that steady state conditions obtain.

The nonlinear polarization third order in the electric fields can then be written

$$\bar{P}^{NL} = A(\bar{E}\cdot\bar{E}^*)\bar{E} + \frac{1}{2}B(\bar{E}\cdot\bar{E})\bar{E}^* \tag{4.4}$$

where, as reviewed in Appendix A,

$$A = 3\{\chi^{(3)}_{1122}(-\omega,\omega,\omega,-\omega) + \chi^{(3)}_{1212}(-\omega,\omega,\omega,-\omega)\}$$

and

$$B = 6\chi^{(3)}_{1221}(-\omega,\omega,\omega,-\omega).$$

The total field within the medium is taken to be

$$\bar{E} = \hat{x}E_1e^{ik_1z} + \hat{x}E_2e^{-ik_2z} + \hat{y}E_3e^{ik_3z} + \hat{y}E_4e^{-ik_4z} + \text{c.c.} \tag{4.5}$$

with a time dependence $\exp(-i\omega t)$ suppressed. This field when used in the nonlinear polarization Eq. (4.4) results in a plethora of cubic terms each of which describes a particular nonlinear process. In the context of degenerate four-wave mixing we retain only those terms that lead to phase-conjugate waves as well as the purely reactive Kerr terms. We also drop terms that vary more rapidly than $\exp(ik_jz)$, where $j = 1,2,3$ or 4. Then using this polarization in the slowly varying envelope equation

$$2ik\frac{d\bar{E}}{dz} = \frac{-4\pi\omega^2\bar{P}^{NL}}{c^2} \tag{4.6}$$

we obtain the model equations:

$$\frac{dE_1}{dz} = i(\alpha+\beta)(|E_1|^2+2|E_2|^2)E_1 + i\alpha(|E_3|^2+|E_4|^2)E_1 + i2\beta E_3E_4E_2^*e^{-i\Delta kz} \tag{4.7a}$$

$$\frac{dE_2}{dz} = -i(\alpha+\beta)(|E_2|+2|E_1|^2)E_2 - i\alpha(|E_3|^2+|E_4|^2)E_2 - i2\beta E_4E_3E_1^*e^{-i\Delta kz} \tag{4.7b}$$

$$\frac{dE_3}{dz} = i(\alpha+\beta)(|E_3|^2+2|E_4|^2)E_3 + i\alpha(|E_1|^2+|E_2|^2)E_3 + i2\beta E_1E_2E_4^*e^{i\Delta kz} \tag{4.7c}$$

$$\frac{dE_4}{dz} = -i(\alpha+\beta)(|E_4|^2+2|E_3|^3)E_4 - i\alpha(|E_1|^2+|E_2|^2)E_4 - i2\beta E_2E_1E_3^*e^{i\Delta kz} \tag{4.7d}$$

where

$$\alpha = \frac{2\pi\omega A}{nc}\ , \qquad \beta = \frac{\pi\omega B}{nc}$$

and $\Delta k = |\bar{k}_1 + \bar{k}_2 - \bar{k}_3 - \bar{k}_4|$.

Except for certain factors of 2 in the Kerr terms resulting from our counterpropagating geometry, this set of equations is identical to that of Armstrong et al [10]. In these

equations the last term on the right hand side gives rise to the four-wave mixing that results in phase-conjugation. The other terms lead to an intensity-dependent propagation constant for each of the four waves.

To solve Eqs. (4.7) we write the fields in terms of their real amplitudes and phases,

$$E_j = a_j e^{i\phi_j} \tag{4.8}$$

and define a relative phase

$$\theta = \Delta kz + \phi_1 + \phi_2 - \phi_3 - \phi_4. \tag{4.9}$$

Then the equations for a_j and θ are

$$\frac{da_1}{dz} = 2\beta a_2 a_3 a_4 \sin\theta \tag{4.10a}$$

$$\frac{da_2}{dz} = -2\beta a_1 a_3 a_4 \sin\theta \tag{4.10b}$$

$$\frac{da_3}{dz} = -2\beta a_1 a_2 a_4 \sin\theta \tag{4.10c}$$

$$\frac{da_4}{dz} = 2\beta a_2 a_1 a_3 \sin\theta \tag{4.10d}$$

$$\frac{d\theta}{dz} = \Delta k + (\alpha+\beta)(a_2^2 - a_1^2 + a_3^2 - a_4^2) + 2\beta\left[\frac{a_3 a_4 a_2}{a_1} - \frac{a_4 a_3 a_1}{a_2} - \frac{a_1 a_2 a_4}{a_3} + \frac{a_2 a_1 a_3}{a_4}\right]\cos\theta. \tag{4.10e}$$

Eqs. (4.10a-d) can be integrated readily. Multiplying (4.10a) by a_1, (4.10c) by a_3, and adding, we obtain

$$\frac{1}{2}\frac{d}{dz}(a_3^2 + a_1^2) = 0. \tag{4.11}$$

Thus we find

$$a_3^2 + a_1^2 = K_a, \text{ a constant.} \tag{4.12a}$$

Similarly, Eqs. 4.10b, c, d lead to

$$a_3^2 - a_2^2 = K_b \tag{4.12b}$$

$$a_3^2 + a_4^2 = K_c, \tag{4.12c}$$

where K_b and K_c are constant. These conservation laws are simply the Manley-Rowe relations of parametric amplifier theory and are a consequence of the fact that the medium is assumed lossless.

To integrate Eq. (4.10e) we use (4.10a-d) to rewrite it as

$$\frac{d\theta}{dz} = \Delta k + (\alpha+\beta)\left(4a_3^2 - (K_a+K_b+K_c)\right) + \left(\frac{d}{dz}\ln a_1a_2a_3a_4\right)\frac{\cos\theta}{\sin\theta} \tag{4.13}$$

Further algebra reduces it to the form

$$\frac{d}{dz}\{a_1a_2a_3a_4\cos\theta - \frac{1}{4\beta}\left((\Delta k-(\alpha+\beta)(K_a+K_b+K_c))a_3^2 + 2(\alpha+\beta)a_3^4\right)\} = 0, \tag{4.14}$$

which yields another constant

$$\Gamma = a_1 a_2 a_3 a_4 \cos\theta - \frac{1}{4\beta}\left[(\Delta k-(\alpha+\beta)(K_a+K_b+K_c))a_3^2+2(\alpha+\beta)a_3^4\right]. \quad (4.15)$$

From (4.15) we find

$$a_1 a_2 a_3 a_4 \sin\theta = \sqrt{(a_1 a_2 a_3 a_4)^2-\{\Gamma+\frac{1}{4\beta}[\Delta k-(\alpha+\beta)K)u+2(\alpha+\beta)u^2]\}^2} \quad (4.16)$$

where $u = a_3^2$ and $K \equiv K_a + K_b + K_c$.

Thus Eq. (4.10c) can be written in terms of a single flux u:

$$\frac{du}{dz} = 4\beta\sqrt{(K_a-u)(u-K_b)(K_c-u)u-\{\Gamma+\frac{1}{4}[\Delta k-(\alpha+\beta)K)u+2(\alpha+\beta)u^2]\}^2} \quad (4.17)$$

The boundary values of the interacting fields are

$$a_1^2(0) = F \qquad a_2^2(L) = B' \qquad (4.18)$$

$$a_3^2(0) = P' \qquad a_4^2(L) = 0 .$$

In addition we specify the unknown value of the transmitted probe field as

$$a_3^2(L) = J' . \quad (4.19)$$

Using these boundary conditions to evaluate the constants K_a, K_b, K_c and Γ, we find

$$K_a = F + P' \quad (4.20a)$$

$$K_b = J' - B' \tag{4.20b}$$

$$K_c = J' \tag{4.20c}$$

$$\Gamma = -\frac{1}{4\beta}\{[\Delta k - (\alpha+\beta)(2J'+F-B'+P')]J' + 2(\alpha+\beta)J'^2\}. \tag{4.21}$$

Finally, we normalize all intensities by F, the intensity of the forward pump wave at the input, so that

$$u \to \frac{u}{F}, \quad B \to \frac{B'}{F}, \quad P \to \frac{P'}{F}, \quad \text{and} \quad J \to \frac{J'}{F}$$

Then Eq. (4.17) can be integrated to give

$$\int_{u(0)=P}^{u(\zeta)} \frac{du}{\sqrt{Q(u;J,P,B,\gamma,\Delta k/4\beta F)}} = 4\beta FL\zeta \tag{4.22}$$

where $\zeta = z/L$, $\gamma = 16\beta^2/(\alpha+\beta)^2$, and

$$Q(u) = \frac{(J-y)}{\gamma}[\gamma(1+P-u)(u-J+B)u - (J-u)(\sqrt{\gamma}\,\frac{\Delta k}{4\beta F} + 2u+B-1-P)^2]. \tag{4.23}$$

Equation (4.22) describes the spatial evolution of the forward probe intensity in the nonlinear medium. To evaluate Eq. (4.22) requires a knowledge of the transmitted probe J. This can be found from the quadrature

$$\int_P^J \frac{du}{\sqrt{Q(u;J,P,B,\gamma,\Delta k/4\beta F)}} = 4\beta FL. \tag{4.24}$$

Details of the procedure are given in Appendix B. In the next section we discuss the physics embodied in Eqs. (4.22) and (4.24).

D. Discussion

The main results of this chapter are contained in Eqs. (4.22) and (4.24). Here the desired quantities (e.g. the transmitted signal) are given implicitly in terms of elliptic integrals whose arguments are functions of these same unknown quantities. In this section we will describe the methods used to obtain meaningful graphical and analytical information from (4.22) and (4.24).

We assume a fixed forward pump intensity at the input of $|E_1(0)|^2 = F$, and recall that all the other intensities are normalized by F. Then the scale of the interaction is determined by a critical length L_c defined by

$$L_c = \frac{\pi}{4\beta F} . \tag{4.25}$$

The motivation for this definition of L_c will become apparent in the discussion of parametric oscillation later in this chapter. Having set L_c, one chooses the normalized quantities B (the backward pump intensity at z = L), P (the probe intensity at the input), $\Delta k L_c$ (the normalized wave vector mismatch), and γ (the nonlinear index parameter defined by $\gamma = 16\alpha^2/(\alpha+\beta)^2$). Then Eq. (4.24) yields the

transmitted probe intensity J as a function of the reduced interaction length L/L_c. The reflected signal intensity $a_4^2(0) = S$ can then be found from the conservation law

$$a_4^2(0) = J - P. \tag{4.26}$$

All other quantities of interest, for example the transmitted forward and backward pump intensities can be found using the Manley-Rowe relations once J is known.

To evaluate Eq. (4.24) we require the roots of the quartic

$$Q(u) = (J-u)\left\{(1+P-u)(u-J+B)u - (J-u)\left(\frac{\Delta k L_c}{\pi} + \frac{2u+B-1-P}{\sqrt{\gamma}}\right)^2\right\} \tag{4.27}$$

These roots $u_1 > u_2 > u_3 > u_4$ are used to transform Eq. (4.24) into a standard Jacobi elliptic integral of the form [16]

$$\frac{\pi L}{L_c} = g\int_0^{\psi} \frac{d\theta}{\sqrt{1 - k^2\sin^2\theta}} \tag{4.28}$$

where

$$g = \frac{2}{\sqrt{(u_1-u_3)(u_2-u_4)}} \tag{4.29}$$

$$\psi = \sin^{-1}\sqrt{\frac{(u_1-u_3)(P-u_2)}{(u_1-u_2)(P-u_3)}}$$

$$k^2 = \frac{(u_1-u_2)(u_3-u_4)}{(u_1-u_3)(u_2-u_4)} \quad . \tag{4.31}$$

The actual value of the integral is calculated using the method of Arithmetic and Geometric Means [17].

The above procedure yields a set of related values for the incident probe P, the transmitted probe J and the reduced interaction length L/L_c. These are then used in (4.22) to obtain an explicit expression for the spatial evolution of the forward probe wave. Rewriting (4.22) as

$$\int_{u(\zeta)}^{J} \frac{du}{\sqrt{Q(u)}} = \frac{\pi L}{L_c}(1-\zeta) \tag{4.32}$$

it is easy to show (see Appendix B) that

$$u(\zeta) = \frac{J - u_1\left(\frac{J-u_3}{u_1-u_3}\right) sn^2\left[\left(\frac{\gamma-4}{\gamma}\right)^{1/2} \frac{\pi L}{gL_c}(1-\zeta)\,\middle|\,k^2\right]}{1 - \left(\frac{J-u_3}{u_1-u_3}\right) sn^2\left[\left(\frac{\gamma-4}{\gamma}\right)^{1/2} \frac{\pi L}{gL_c}(1-\zeta)\,\middle|\,k^2\right]} \tag{4.33}$$

where sn is a Jacobian elliptic function. Since sn is a periodic function of its arguments, the intensities of the interacting waves will, in general, oscillate in space. The period of these oscillations depends on the transmitted probe intensity and is given by twice the complete elliptic integral

$$K(k) = \int_0^{\pi/2} \frac{d\theta}{\sqrt{1 - k^2 \sin^2\theta}} \qquad (4.34)$$

where k has been defined previously.

The quartic polynomial Q can be associated with a potential

$$V(u) = -Q(u)$$

and the related equation of motion (4.17). This potential is shown in Fig. (4.2) for a particular set of input and output intensities. The point $u_2 = J$ is one of the turning points of this potential. Since the intensity u is a positive quantity, it is constrained to lie between the roots u_3 and u_2. If the interaction length is chosen to maximize the transmitted probe intensity, this intensity J_m can be found by solving

$$Q(u=P; J_m) = 0,$$

i.e. u = P should be a turning point of the potential. Thus we find

$$J_m = P + \frac{PB}{P + \left[\frac{\Delta k L_c}{\pi} + \frac{B+P-1}{\sqrt{\gamma}}\right]^2} \; . \qquad (4.35)$$

We note that if the input probe P = 0, then $J_m = 0$ unless the condition

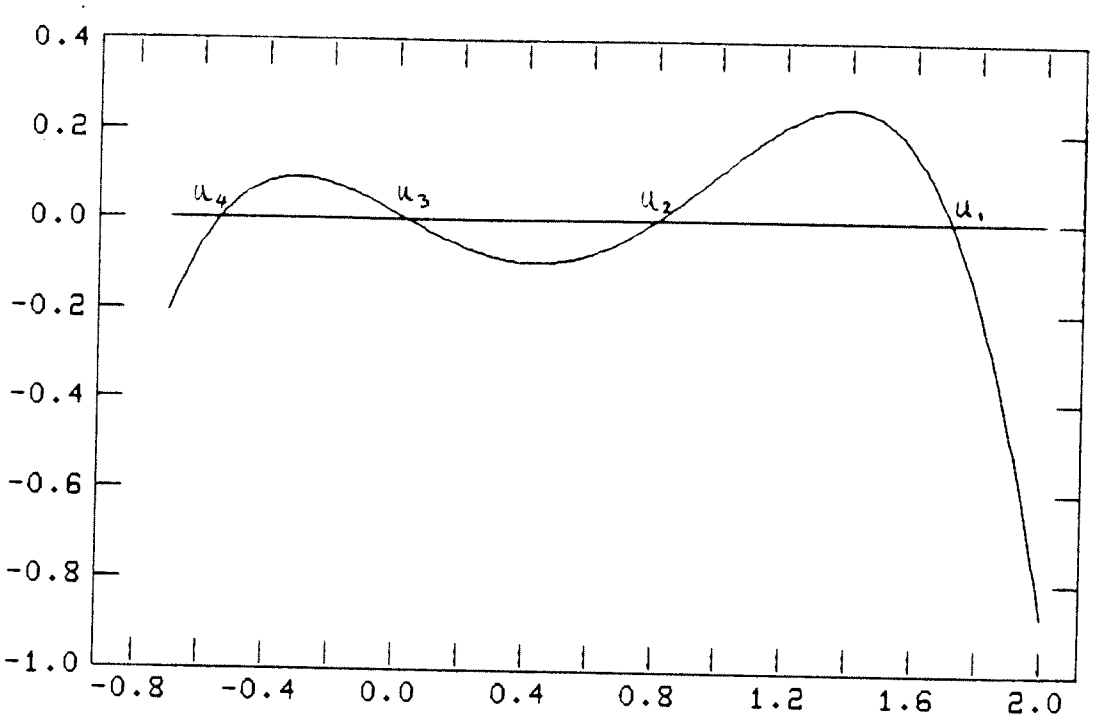

Fig. (4.2): Quartic potential for the forward probe flux in DFWM. Here F = B = 1, P = 0.4 and J = 0.8.

$$\frac{\Delta k L_c}{\pi} + \frac{B-1}{\sqrt{\gamma}} = 0 \qquad (4.36)$$

is satisfied. When Eq. (4.36) holds then there is an output signal of maximum intensity

$$J_m = B$$

even in the absence of an input probe. This is the oscillation phenomenon mentioned by Pepper and Yariv [18].

A physically interesting special case is when the phase mismatch Δk is sufficiently large that the signal waves do not grow to an appreciable magnitude. In that case we may drop the purely reactive Kerr terms in Eqs. (4.7). This is equivalent to setting $\alpha = -\beta$ in (4.10e) or $\gamma = \infty$ in all the results of the last section.

These solutions are shown in Figs. (4.3). In curve (a), $\Delta k L_c = \pi$ and we find that the transmitted probe intensity oscillates as a function of the reduced interaction length. Because of the large phase mismatch, the signal and probe intensities do not grow very large. In curve (c), $\Delta k L_c = 0$, the growth of the transmitted (reflected) signal is monotonic and complete conversion results.

We have seen that the presence of a phase mismatch in four-wave mixing leads to signal intensities that vary periodically with interaction length. In the limit of zero phase mismatch, the period of these oscillations is infinite, hence the evolution of the signal wave is monotonic.

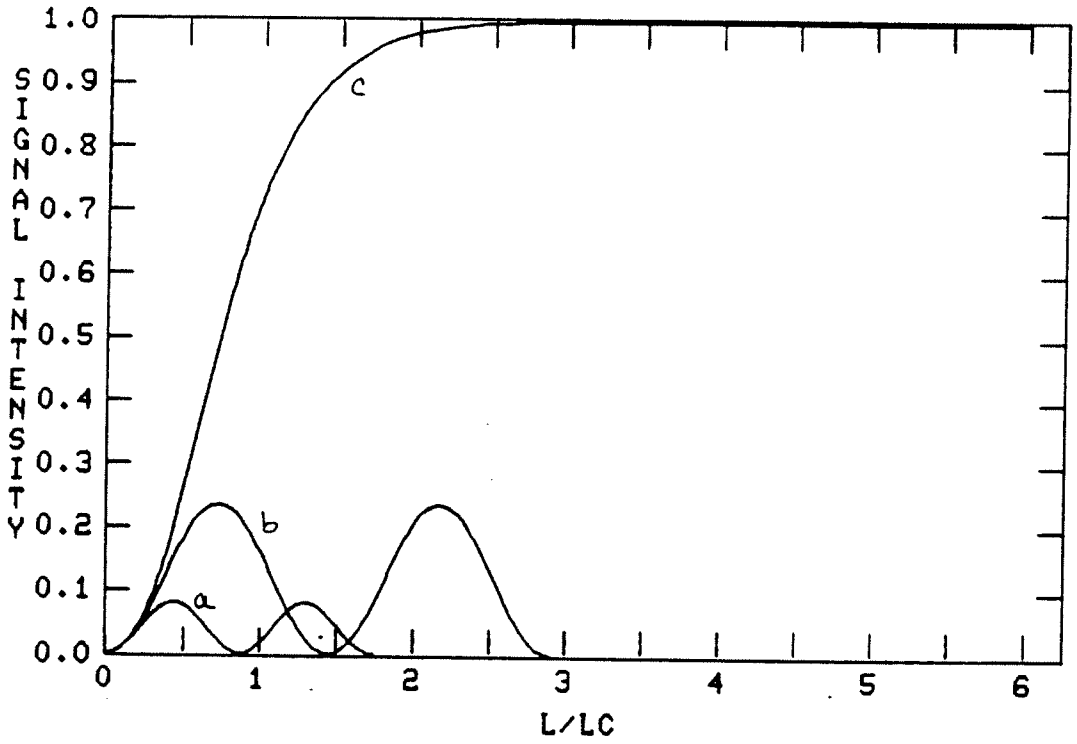

Fig. (4.3): Effect of a finite phase-mismatch on DFWM without Kerr effect. (a) $\Delta\kappa L_c = 2$, (b) $\Delta\kappa L_c = 1$, (c) $\Delta\kappa L_c = 0$. Here $p = 0.4$, $F = B = 1$.

We now include the previously neglected Kerr terms and find that even when there is "perfect" phase-matching ($\Delta k = 0$), the signal intensity still oscillates as a function of L. This is due to the quadratic Kerr effect which makes the phase velocities of the interacting waves dependent on their amplitudes. Thus as the amplitudes vary through the four-wave mixing interaction, the nonlinear phase-breaking leads to an effective coherence length. The most interesting discovery here is that these spatial oscillations are highly nonlinear and can become multivalued. For the same input intensities and interaction length there are three possible solutions for the signal intensity. This leads to the intriguing possibility of hysteresis and bistability in degenerate four-wave mixing.

Consider the dependence of the reflected (or transmitted) signal on the reduced interaction length L/L_c. Since $L_c = \pi/4\beta F$ and F is the incident pump intensity, L/L_c can also be regarded as the nonlinear phase shift due to the pump. We note however that since all the other intensities are normalized by F, it is appropriate to consider F fixed and to treat the variation in L/L_c ($= 4\beta FL/\pi$) as due solely to changes in length. Fig. (4.4) shows the reflected signal intensity as a function of L/L_c for several values of the normalized probe intensity P. These curves were obtained from Eq. (4.24) using methods discussed more fully in Appendix B. The results are for

zero phase-mismatch ($\Delta kL_c = 0$) and equal forward and backward pump intensities. The parameter γ which measures the strength of the four-wave mixing interaction relative to the Kerr effect is chosen to be 8.14 as appropriate for CS_2[1]. In each case we see that the reflected signal grows in intensity as the interaction length is increased until it reaches a maximum intensity given (from Eq. (4.35)) by

$$S_m = \frac{PB}{P + \left[\frac{\Delta kL_c}{\pi} + \frac{B+P-1}{\sqrt{\gamma}}\right]^2}, \tag{4.37}$$

at a point

$$L_m/L_c = \frac{\sigma}{\pi}^{1/2} gK(k), \tag{4.38}$$

where $\sigma = \gamma/(\gamma-4)$ and k is defined in Eq. (4.31). It is clear from Fig. (4.4) that for some range of L/L_c, the reflected signal intensity may exceed that of the probe. Defining the maximum gain as

$$G_{max} = S_m/P ,$$

we find that for $P<<\gamma$, Eq. (4.37) shows that G_{max} is inversely proportional to the probe intensity. This is because a weak incident probe can draw more energy from the pump before depletion occurs.

After the signal attains its maximum, a further increase in L/L_c causes the signal intensity to decrease as

the pump is regenerated. This drop in intensity can be continuous (as in the first lobe of curve (c), or discontinuous (as in (a) and (b)). The discontinuous transitions occur in the regions where the S vs L/L_c curve is multivalued. In such cases, one or more of the steady state solutions is unstable and is thus physically inaccessible. Our steady state analysis does not permit us to say which of the three solutions is unstable. A proper treatment of the stability problem will require a numerical solution of the full time-dependent four-wave mixing equations. Damping mechanisms such as absorption and a finite material relaxation time will have to be taken into account. For the rest of this discussion however, we will assume as is usually done when multivalued solutions exist [19], that the negative slope regions are unstable. Then as the interaction length is varied, the reflected signal will trace out the hysteresis loops marked by arrows in Fig. (4.4). The nulls in the signal intensity are equally spaced by a length $L = 2L_c$.

The hysteresis phenomena observed here depend on the feedback produced by the counterpropagating waves as they set up gratings within the nonlinear medium. A measure of the strength of feedback is the relative intensities of the forward and backward pump waves. It is to be expected that as the intensity of the backward pump wave is reduced relative to the forward pump the hysteresis should become

Fig. (4.4): Phase-matched degenerate four-wave mixing with Kerr effect included. Transmitted probe vs. reduced interaction length L/L_c. Here $F = B = 1$, $\Delta kL_c = 0$. Probe values: (a) $P = 0.2$ (b) $P = 0.4$ (c) $P = 0.8$.

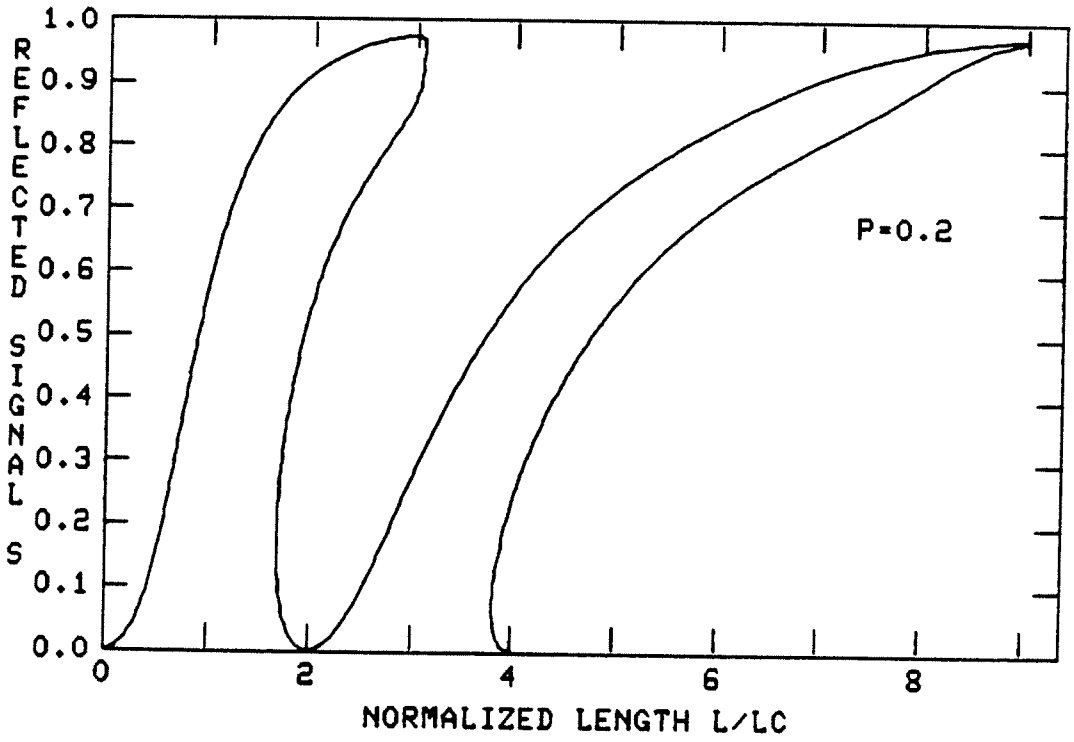
REFLECTED SIGNALS
1.0
0.9
0.8
0.7
0.6
0.5
0.4
0.3
0.2
0.1
0.0
0
2
4
6
8
NORMALIZED LENGTH L/LC
P=0.2

Fig. (4.4a)

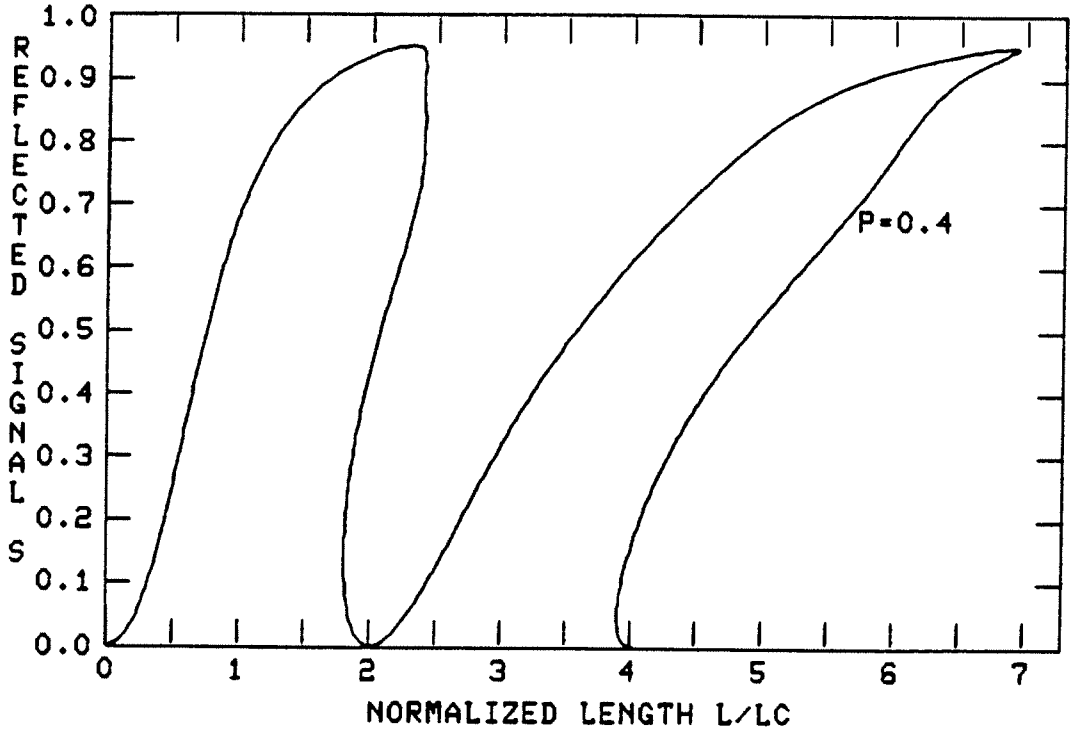
REFLECTED SIGNALS
1.0
0.9
0.8
0.7
0.6
0.5
0.4
0.3
0.2
0.1
0.0
0
1
2
3
4
5
6
7
NORMALIZED LENGTH L/LC
P=0.4

Fig. .(4.4b)

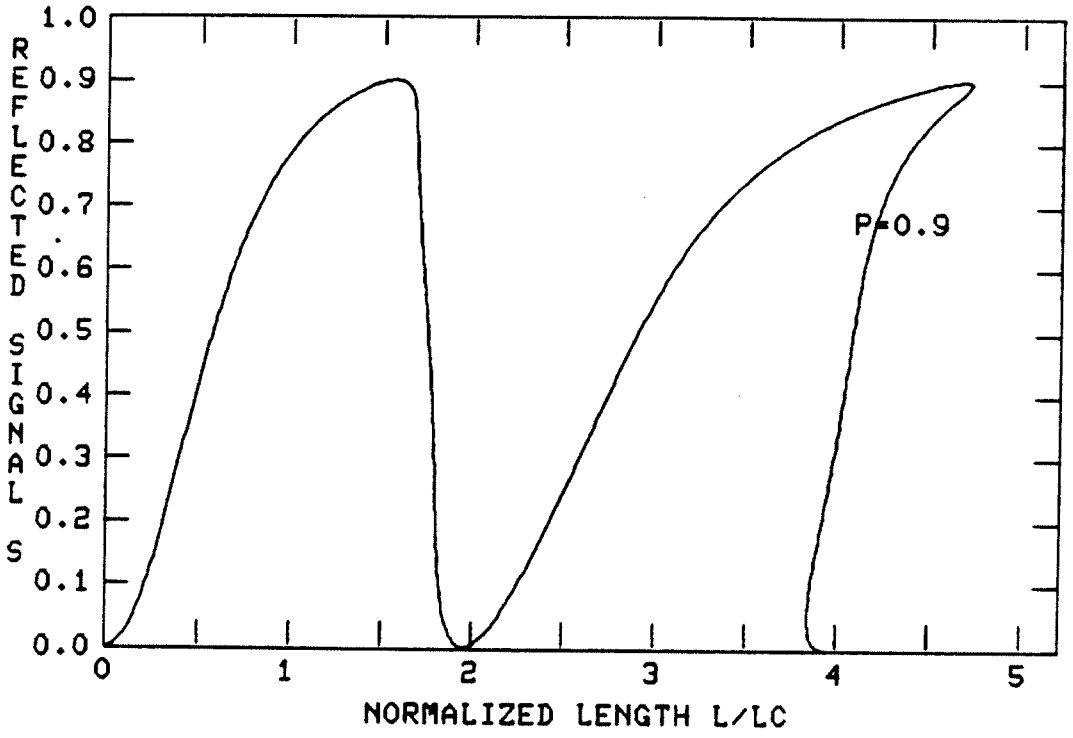
REFLECTED SIGNALS
1.0
0.9
0.8
0.7
0.6
0.5
0.4
0.3
0.2
0.1
0.0
0
1
2
3
4
5
P=0.9
NORMALIZED LENGTH L/LC

Fig. (4.4c)

less pronounced. Fig. (4.5) shows the reflected signal versus the L/L_c for several values of the backward pump intensity B. The probe intensity is set at 0.4. We see that as B is reduced, the region of hysteresis shrinks until it disappears altogether for $B \lesssim .5$. The largest hysteresis effects are obtained when the backward and forward pump intensities are equal. When F and B are unequal, the standing wave they create is not fully modulated, and in addition the intensity dependent refractive index leads to a phase mismatch proportional to F - B. This leads to a reduction in the reflected signal intensity and in the hysteresis width.

When forward and backward pump intensities are equal, any phase mismatch similarly leads to a reduction in conversion efficiency and a reduction in the width of the hysteresis loop. This is shown in Fig. (4.6) where we plot S versus L/L_c for several values of ΔkL_c.

The spatial distribution of the four interacting waves can be found from Eq. (4.33) and the Manley-Rowe relations. We first pick a value for L/L_c and then read off the corresponding values of P, B and J (or S) from the appropriate curve in Fig. (4.3). These are then used in Eq. (4.33) to find the intensity of the forward-going probe wave u as a function of $\zeta = Z/L$. The intensity distribution for the backward signal then follows from Eq. (4.12c). Fig. (4.7) shows the forward intensity distributions for a

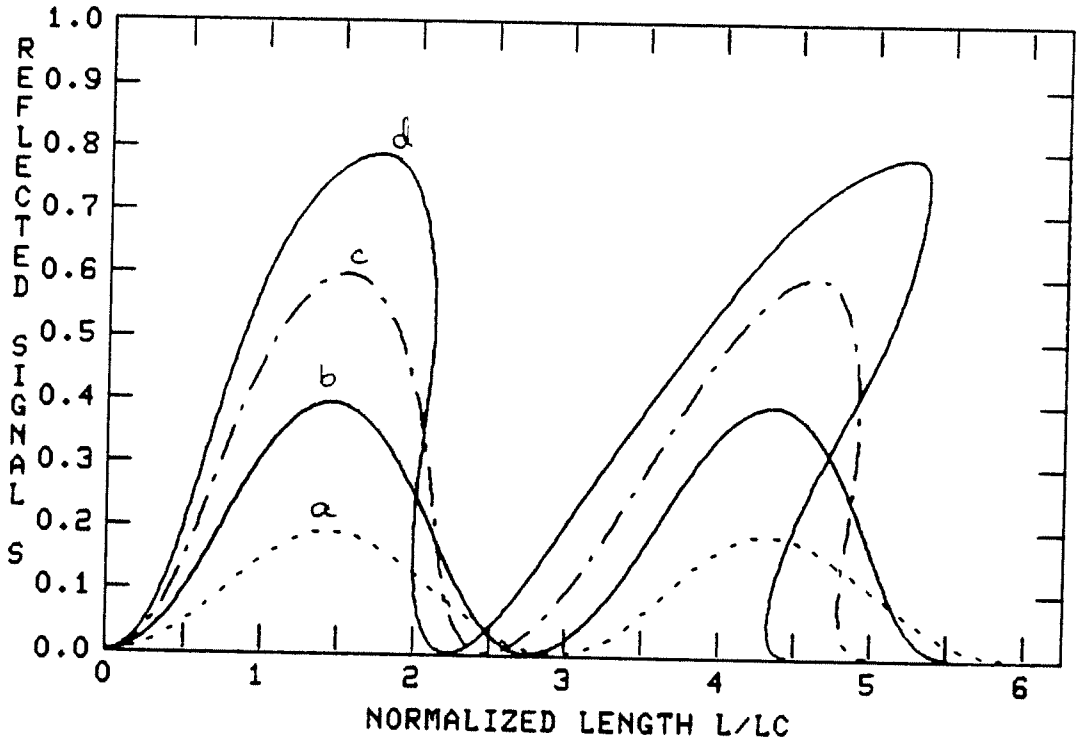

Fig. (4.5): Reflected signal vs. L/L_c for several values of backward pump intensity. Here F = 1, P = 0.4, and (a) B = 0.2 (b) 0.4 (c) 0.6 (d) 0.8.

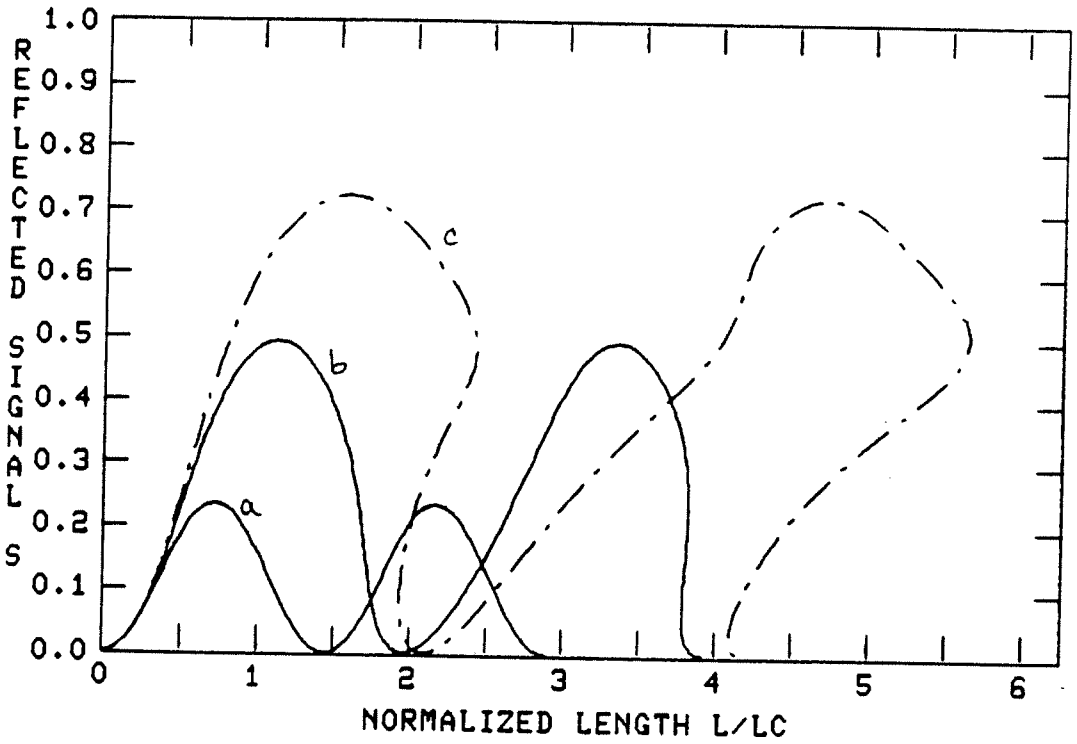

Fig. (4.6): Effects of a finite phase mismatch. Reflected signal vs. L/L_c for several values of phase mismatch. (a) $\Delta\kappa L_c = 2$ (b) 1 (c) 0.5.

value of L/L_c chosen to lie in the hysteresis region of Fig. (4.3). For the same value of probe intensity there are three possible intensity distributions of the reflected signal. The corresponding forward probe intensity distributions are shown in Fig. (4.8).

We have seen that the four-wave mixing interaction can give rise to an amplified reflected signal. It is in essence a four-photon parametric amplifier. Given sufficient feedback, parametric amplifiers become parametric oscillators. Above a certain pump threshold parametric oscillators emit an oscillation signal without any probe input. Here we will use the small-signal theory to obtain the oscillation threshold in degenerate four-wave mixing. This is valid since at the threshold, the signal amplitude builds up from the noise level. The final signal amplitude is limited by pump depletion and hence the nonlinear theory is necessary for finding this amplitude.

The small-signal theory gives

$$\frac{dE_3}{dz} = i2\beta E_1 E_2 E_4^* \ , \tag{4.39}$$

$$\frac{dE_4}{dz} = -i2\beta E_1 E_2 E_3^* \ , \tag{4.40}$$

where the pump intensities are assumed constant. These equations are readily solved to give

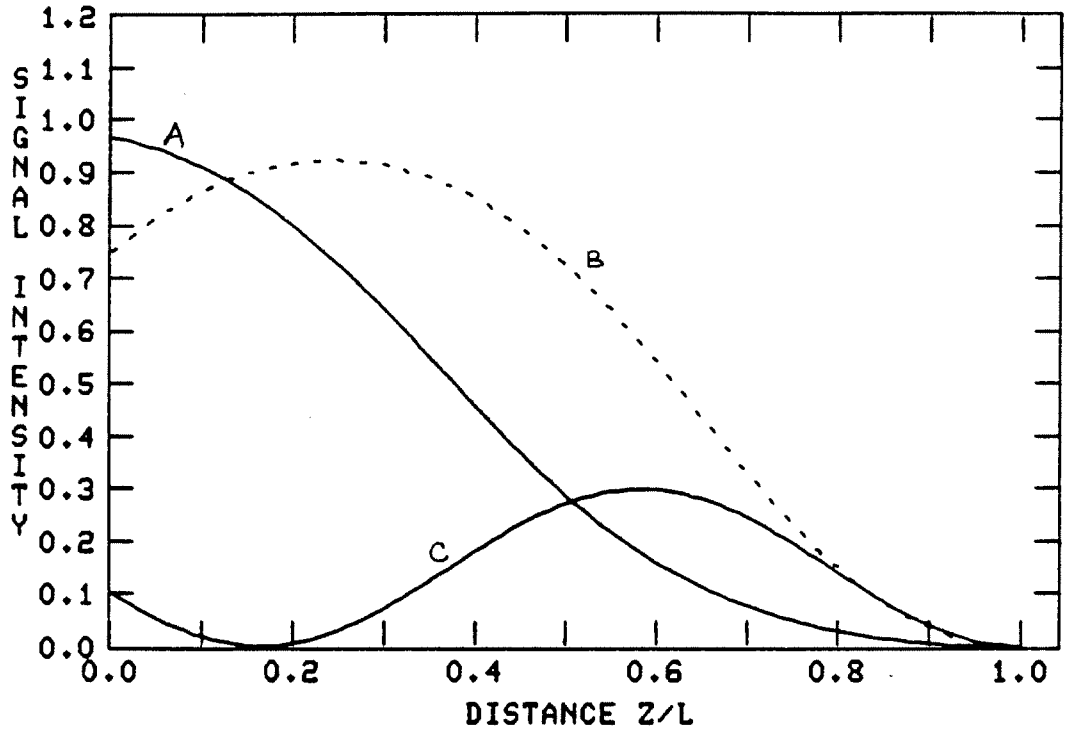

Fig. (4.7): Spatial distributions of the backward signal intensity for $L/L_c = 1.8$. Here $F = B = 1$, $\Delta\kappa L_c = 0$ and $P = 0.2$.

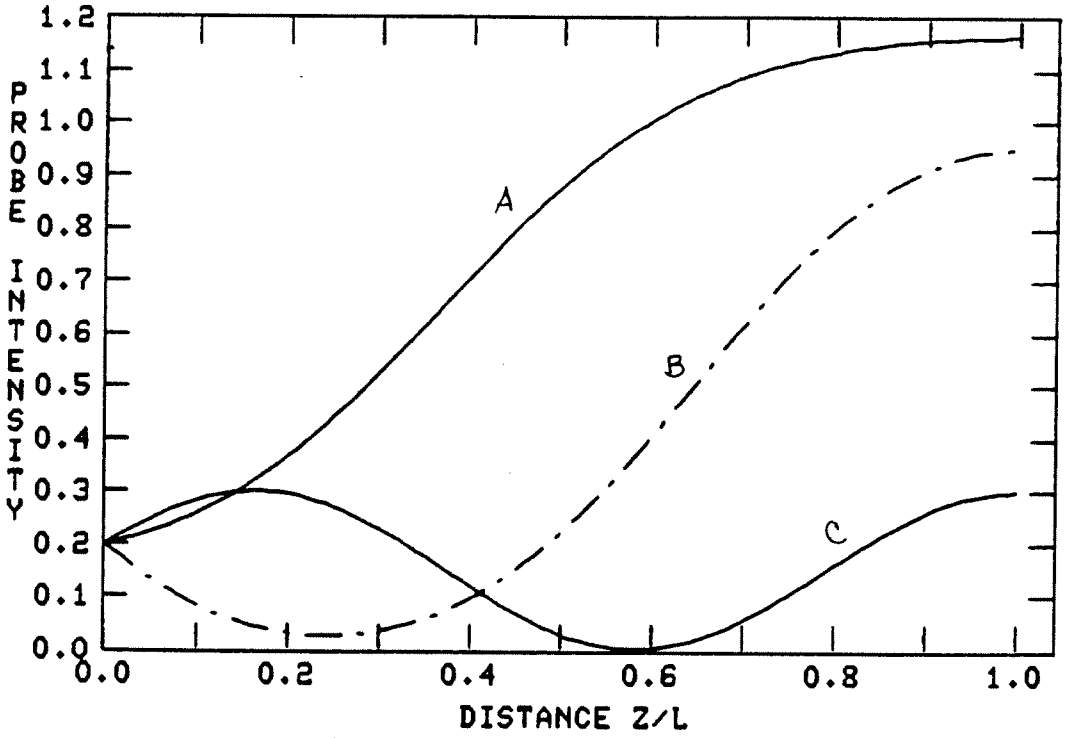

Fig. (4.8): Spatial evolution of the forward probe intensity.

$$\frac{|E_4(0)|^2}{|E_3(0)|^2} = \tan^2(2\beta FL). \qquad (4.41)$$

where $F = E_1 E_2$. We see that when $2\beta FL = \pi/2$, the signal gain is infinite, so that an oscillation signal exists without any probe input. We thus define a critical length

$$L_c = \frac{\pi}{4\beta F}$$

at which oscillation begins. This is the same point at which oscillation occurs in the nonlinear theory. The amplitude of the oscillation signal is found from the nonlinear analysis by setting the probe equal to zero in Eq. (4.32). This solution is shown in Fig. (4.9). The corresponding spatial distribution of signal intensity is found from Eq. (4.33) and is shown in Fig. (4.10).

For a fixed pump intensity we can infer the relationship between signal and probe intensities from Eq. (4.33). As shown in Fig. (4.11), at low pump intensities the signal increases linearly with the probe intensity. Above the critical pump intensity, oscillation occurs and it is possible to have a signal without an input probe. By now increasing the probe intensity from zero it is possible to quench the state of oscillation as pump depletion occurs. The pump can no longer sustain oscillation at that level and the output drops discontinuously to a low value. As

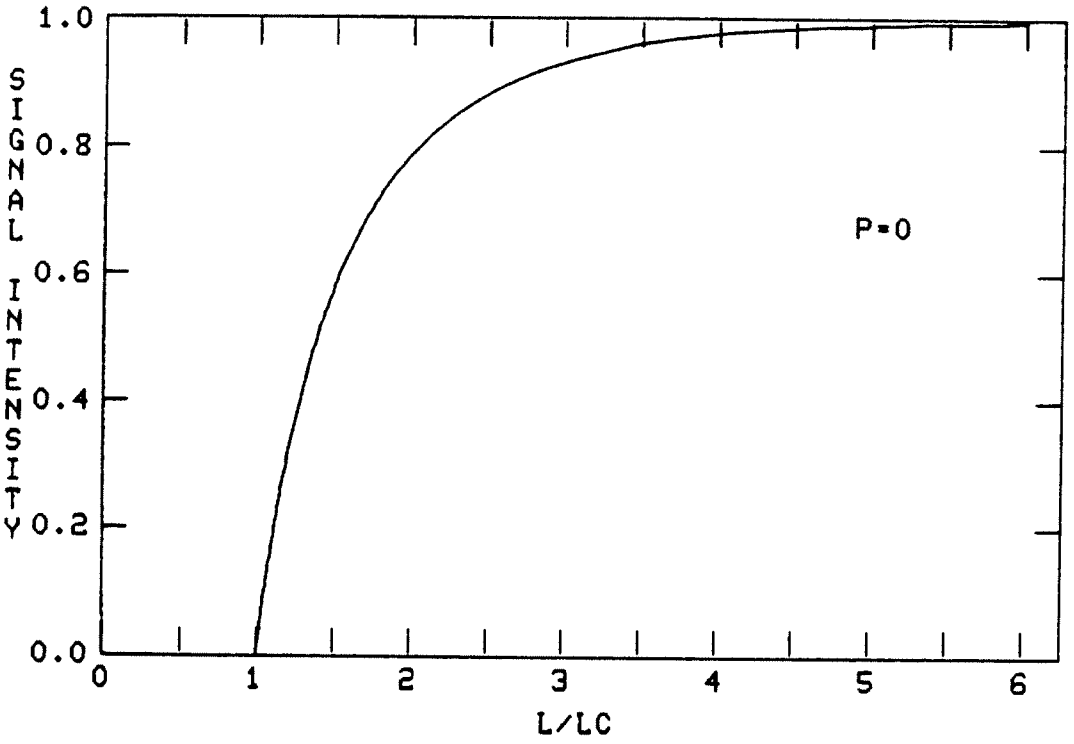

Fig. (4.9): Oscillation signal in DFWM. Forward and backward pump intensities are equal, and there is no incident probe.

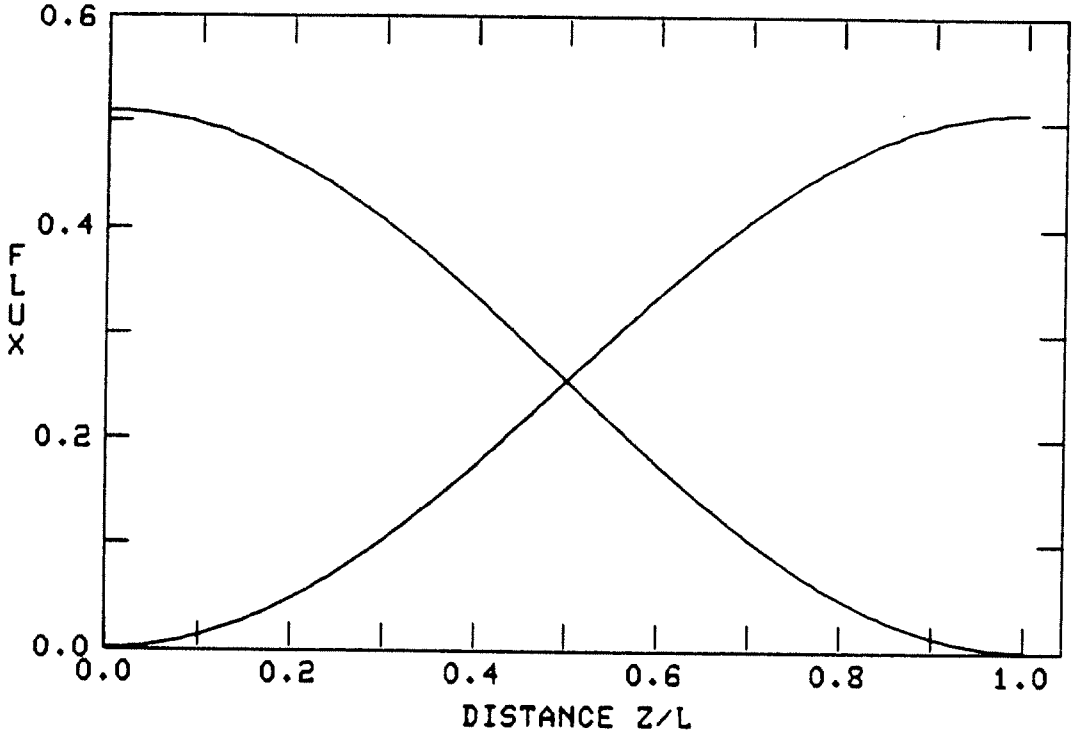

Fig. (4.10): Spatial evolution of signal waves under oscillation conditions. Here $L/L_c = 1.4$.

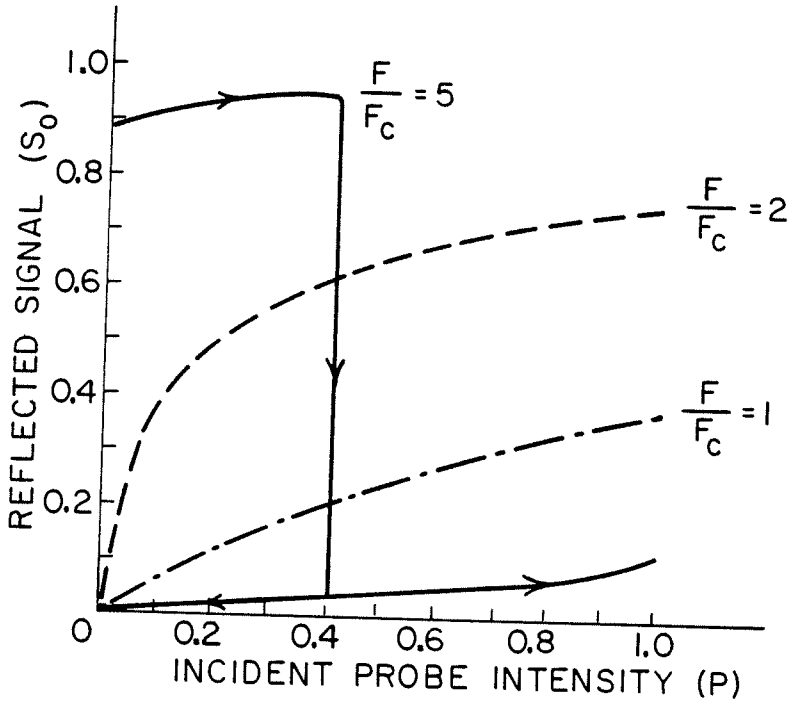

Fig. (4.11): Reflected signal vs. incident probe intensity for three values of pump intensity. Here $F/F_c = \pi L/\sigma^{1/2}L_c$.

the probe is reduced the signal stays at this low value until the probe intensity goes to zero. It is likely that this point is metastable and that once the probe dips below the noise level, oscillation will start up again.

E. Experimental Considerations

In this section we discuss the experimental conditions under which the phenomena predicted here may be observed.

In making numerical estimates of the intensities required for these nonlinear effects the crucial quantity is the reduced interaction length $4\beta FL$. When this quantity is on the order of π, the interesting phenomena of self-oscillation and hysteresis begin to manifest themselves. To satisfy this condition one requires media with high nonlinearities, and an interaction region L sufficiently long that the required critical power F is not excessive. We consider three different media with large nonlinear indices: a gas -- Na vapor, a liquid -- CS_2 and a solid -- InSb.

In Na vapor resonance enhancement leads to values of $\chi^{(3)}$ on the order of 10^{-8}esu [20]. With an interaction length of 5 cm, the effect of an intensity-dependent refractive index on the efficiency of DFWM was observed at modest pump powers of $40kW/cm^2$. In their experiments Liao et al. observed that as the pump intensity was increased, the signal intensity grew to a maximum, saturated, and then began to decrease with further increases of pump intensity.

To demonstrate bistability through four-wave mixing in sodium vapor would require an interaction length of at least 10 cm and pump intensities on the order of $100kW/cm^2$. One possible experiment would be to vary the optical length of the medium by changing its pressure and looking for hysteresis in the reflected signal.

Since the critical intensity is of the same order as the threshold for whole-beam self focussing, care must be taken to prevent the latter process from occurring. This may be accomplished by carrying out the four wave interaction in an optical fiber. CW degenerate four-wave mixing has been observed by Au Yeung et al. in a 3m long fiber filled with CS_2. There the pump power used was only 6mW.

InSb has one of the largest $\chi^{(3)}$'s ever measured. At 77°K and at a wavelength of 5.3μ, $\chi^{(3)} \sim 10^{-2} - 10^{-1}$ esu in InSb. This makes it an attractive candidate for observing bistability in DFWM. Due to its high index of refraction however it will be difficult to eliminate the Fresnel end reflections which will tend to obscure the effect. Assuming that the end-reflections could be successfully eliminated, one might observe these nonlinear "Maker fringes" by varying the optical length of the sample thermally. Alternatively, one could use a wedge-shaped sample which is translated laterally through the counterpropagating beams. For a 1mm long sample, the required critical power is on the order of 20mW.

REFERENCES -- CHAPTER IV

1. J.H. Marburger and J.F. Lam, "Nonlinear theory of degenerate four-wave mixing," Appl. Phys. Lett., vol. 34, p. 389, 1979.
2. For a review of applications of degenerate four-wave mixing see R.W. Hellwarth, IEEE J. Quantum Electron. vol. QE-15, p. 101, 1979.
3. P.D. Maker and R.W. Terhune, "Study of optical effects due to an induced polarization third order in the electric field strength," Phys. Rev., vol. 137, p. A801, 1965.
4. R.W. Hellwarth, "Generation of time-reversed wave fronts by nonlinear refraction," J. Opt. Soc. Am., vol. 67, p. 1, 1977.
5. H.G. Winful and J.H. Marburger, "Hysteresis and optical bistability in degenerate four-wave mixing," Appl. Phys. Lett., vol. 36, p. 613, 1980.
6. V.S. Letokhov and B.D. Pavlik, "Theory of the resonant-feedback laser," Sov. Phys. -- Tech. Phys., vol. 13, p. 251, 1968.
7. B.Ya. Zeldovich, "Some features of stimulated scattering of light," Sov. J. Quantum Electron., vol. 7, p. 525, 1977.

8. S.A. Akhmanov and G.A. Lyakhov, "Effects of inhomogeneity of optical pumping in lasers and in stimulated scattering. Self-excitation due to distributed feedback," Sov. Phys.-JETP, vol. 39, p. 43, 1974.

9. G.A. Lyakhov and Yu.V. Ponomarev, "Steady-state nonlinear stimulated emission from a laser with a distributed feedback," Sov. J. Quant. Electron, vol. 6, p. 57, 1976.

10. J.A. Armstrong, N. Bloembergen, J. Ducuing and P.S. Pershan, "Interaction between light waves in a nonlinear dielectric," Phys. Rev., vol. 127, p. 1918, 1962.

11. A recent review of four-wave mixing spectroscopy is by M.D. Levenson, in Physics Today, vol. 30, p. 45, 1977.

12. S.M. Jensen and R.W. Hellwarth, "Generation of time-reversed waves by nonlinear refraction in a waveguide," Appl. Phys. Lett., vol. 33, p. 404, 1978.

13. D.M. Bloom and G.C. Bjorklund, "Conjugate wave-front generation and image reconstruction by four-wave mixing," Appl. Phys. Lett., vol. 31, p. 592, 1977.

14. A. Yariv, "Four-wave nonlinear optical mixing as real time holography," Opt. Comm. 25, 23 (1978).

15. J.H. Marburger and J.F. Lam, "Effect of nonlinear index changes on degenerate four-wave mixing," Appl. Phys. Lett.

16. P.F. Byrd and M.D. Friedman, Handbook of Elliptic Integrals for Engineers and Scientists. New York: Springer-Verlag, 1971.

17. M. Abramowitz and I.A. Stegun, Handbook of Mathematical Functions. Washington, DC: U.S. Government Printing Office, 1964.

18. A. Yariv and D.M. Pepper, "Amplified reflection, phase conjugation and oscillation in degenerate four-wave mixing," Opt. Lett., vol. 1, p. 16, 1977.

19. N. Minorsky, Nonlinear Oscillations. Princeton, NJ: van Nostrand Co., 1962.

20. D.M. Bloom, N.P. Economou, and P.F. Liao, "Observation of amplified reflection by degenerate four-wave mixing in atomic sodium vapor," Opt. Lett., vol. 2, p. 158, 1978.

21. J.Au Yeung, D. Fekete, D.M. Pepper, A. Yariv, and R.K. Jain, "Continuous backward-wave generation by degenerate four-wave mixing in optical fibers," Opt. Lett., vol. 4, p. 42, 1979.

22. D.A.B. Miller, R.G. Harrision, A.M. Johnston, C.T. Seaton and S.D. Smith, "Degenerate four-wave mixing in InSb at 5K," Opt. Commun., vol. 32, p. 478, 1980.